JOURNAL OF APPLIED ELECTROCHEMISTRY 19 (1989) 448–452

# High-temperature $C_1$-gas fuel cells using proton-conducting solid electrolytes

H. IWAHARA, H. UCHIDA, K. MORIMOTO, S. HOSOGI

*Department of Environmental Chemistry and Technology, Faculty of Engineering, Tottori University, Koyamacho, Tottori 680, Japan*

Received 7 June 1988; revised 10 November 1988

With proton-conducting solid electrolytes based on $SrCeO_3$ or $BaCeO_3$, high-temperature fuel cells were constructed and cell performances were examined. Mixtures of water vapor and some $C_1$ gases such as methanol vapor or methane were used as fuel by internal reforming to liberate hydrogen in the anode compartment. These fuel cells worked stably above 900° C. Addition of water vapor to the fuel was necessary to prevent carbon deposition at the anode. The performances of the cells were limited mainly by ohmic resistance of the solid electrolyte.

## 1. Introduction

Recently, solid oxide fuel cells (SOFC) have been intensively studied. While oxide ion conductors like stabilized zirconias have been mainly used as an electrolyte material, high-temperature-type proton-conducting solids are also favorable materials as a solid electrolyte for fuel cells. Several years ago, we discovered high-temperature proton-conducting solids based on $SrCeO_3$ or $BaCeO_3$ [1, 2] and fabricated fuel cells using these ceramics as the solid electrolytes [1–7]. The fuel cells worked stably at 800–1000° C.

The wide choice of possible fuels is one of the excellent advantages for both SOFC and MCFC (molten carbonate fuel cell). Much attention is being devoted to 'internal reforming'-type fuel cells [8–10]. For proton-conductor fuel cells, various fuels which liberate hydrogen at high temperatures are also available [6]. In this study we examine the performances of $C_1$-gas fuel cells using high-temperature-type proton-conducting solid electrolytes based on $SrCeO_3$ or $BaCeO_3$. Mixtures of water vapor and some $C_1$ gases such as methanol vapor and methane were used as the fuel.

## 2. Experimental details

The solid proton conductors used in this experiment were $SrCe_{0.95}Yb_{0.05}O_{3-\alpha}$ and $BaCe_{0.90}Nd_{0.10}O_{3-\alpha}$ ($\alpha$ is the number of oxygen deficiencies per perovskite-type unit cell). The construction of the solid electrolyte fuel cell was the same as in ref. [2]. The dense sinters obtained were sliced into thin discs (thickness: about 0.5 mm; diameter: 12 mm). Porous platinum electrodes were attached to both faces of the electrolyte disc (projected area: 0.5 or 0.28 $cm^2$). A platinum wire was wound around the side of the disc as the reference electrode. The electrode compartments were separated by the ceramic electrolyte and each compartment was sealed by a glass ring gasket.

Air or oxygen was introduced to the cathode compartment. To the anode compartment, methane or methanol vapor was supplied with water vapor to prevent carbon deposition. When methanol vapor was used as the fuel, we employed either argon carrier gas saturated with aqueous methanol at a given temperature, or a vaporizer heated by an electric furnace as shown in Fig. 1. After removal of residual water vapor by a condenser, the exhaust gas from the anode compartment was analyzed by a gas chromatograph (Shimazu, Model GC 3BT, carrier gas: argon). As the column packing, Porapak Q ($CO_2$, $C_2H_4$, $C_2H_6$) and molecular sieve 5 A ($H_2$, $O_2$, $N_2$, $CH_4$, CO) were used. A thermal conductivity detector and an automatic integrator (SIC, Chromatocorder, Model 11) were employed.

The polarization characteristics of the electrodes were studied by a current-interruption method [5].

## 3. Results and discussion

### 3.1. *Methane fuel cell*

Using an $SrCe_{0.95}Yb_{0.05}O_{3-\alpha}$ disc as the electrolyte, we fabricated a methane fuel cell. Typical discharge performances are shown in Fig. 2. Below 800° C, the terminal voltage was unstable since methane was hardly pyrolyzed and hydrogen concentration was very low. At low vapor content the cell performance was not so stable, but an addition of vapor stabilized the performance. Above 100 Torr of vapor pressure, the current output was steady and the relation between the terminal voltage and the current density was linear at 900–1000° C. Figure 3 shows the change in terminal voltage in the continuous discharge test at 70 mA $cm^{-2}$ at 1000° C. The fluctuations in the terminal voltage were attributed to the turbulence of the fuel flow occurring in the gas sampling for analysis or in the condensation of water vapor at the outlet from the cell. The cell performance did not deteriorate after 8 h of test. Although a further long discharge test run may



0021-891X/89 $03.00 + .12 © 1989 Chapman and Hall Ltd.

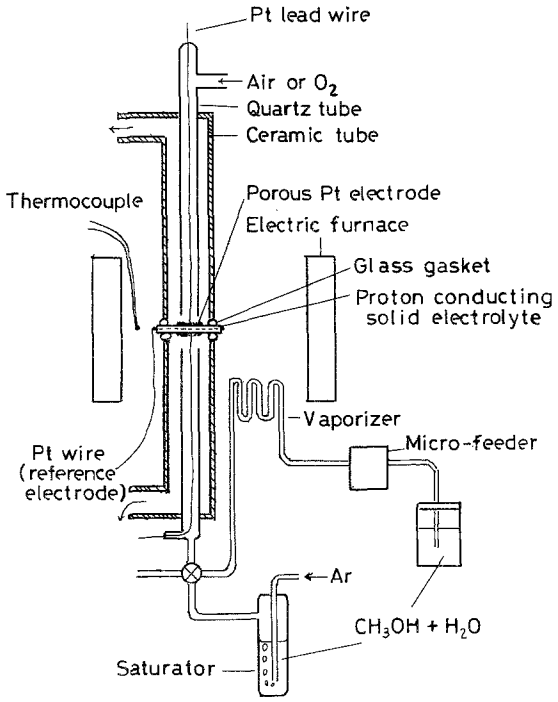


Fig. 1. Schematic diagram of experimental methanol fuel cell.

be necessary for practical use, the above results show that $SrCeO_3$-based ceramic works as a stable electrolyte for a methane fuel cell.

Exhaust gas from the anode compartment was analyzed by gas chromatography. Typical results are shown in Table 1. The exhaust gas contained $H_2$, CO, $CO_2$ and unreacted $CH_4$. We also detected trace amounts of $C_2H_4$ and $C_2H_6$, which were formed by a coupling reaction of methane. This indicates that various pyrolysis reactions occur in the anode compartment.

$$CH_4 + H_2O \longrightarrow 3H_2 + CO \quad (1)$$

$$CO + H_2O \rightleftharpoons H_2 + CO_2 \quad (2)$$

$$CH_4 \longrightarrow 2H_2 + C \quad (3)$$

$$C + H_2O \longrightarrow H_2 + CO \quad (4)$$

$$2CH_4 \longrightarrow C_2H_6 + H_2 \quad (5)$$

$$2CH_4 \longrightarrow C_2H_4 + 2H_2 \quad (6)$$

At 1000° C, since the $H_2$/CO ratio in the exhaust gas was about 3 at open-circuit conditions, Equation 1 might be dominant in the anode compartment. Judging from the mass balance of carbon, the amount of carbon deposited in the anode compartment decreases with increasing $P_{H_2O}$.

*Table 1. Composition of exhaust gas from fuel compartment at open circuit: $CH_4 + H_2O$, Pt $|SrCe_{0.95}Yb_{0.05}O_{3-\alpha}|$ Pt, air ($CH_4$ flow rate = 30 ml min$^{-1}$, $P_{H_2O}$ in fuel = 300 Torr)*

| Cell temp. (° C) | Composition (%) | | | | | |
|---|---|---|---|---|---|---|
| | $H_2$ | CO | $CO_2$ | $C_2H_4$ | $C_2H_6$ | $CH_4$ |
| 900 | 20.0 | 4.8 | 2.5 | 0.02 | trace | 68.9 |
| 1000 | 31.6 | 9.4 | 3.8 | 0.09 | trace | 53.4 |

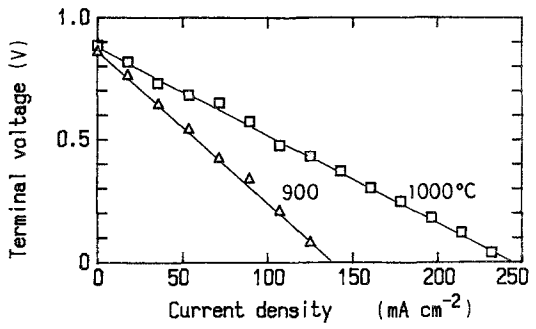


Fig. 2. Performance of the methane fuel cell; $CH_4 + H_2O$, Pt$|SrCe_{0.95}Yb_{0.05}O_{3-\alpha}|$Pt, air ($CH_4$ flow rate = 30 ml min$^{-1}$, $P_{H_2O}$ in fuel = 300 torr, electrolyte thickness = 0.50 mm).

Figure 4 shows the polarization characteristics for each electrode, measured by the current-interruption method. At 1000° C, the polarizations were very small, while below 900° C a relatively large polarization was observed at the cathode, probably due to diffusion limitation of adsorbed oxygen atoms [5]. Since the ohmic drop was large compared to the residual voltage drop on current interruption, the cell performance depends mainly on the resistance of the solid electrolyte as observed in our previous fuel cells [1–7].

The effect of discharge current on the composition of exhaust gas is not so clear, since the electrode area is small and the current is not so high (that is, utilization of the fuel by the cell reaction is low). However, it can be expected that ethane or ethylene may be produced by a coupling reaction of $CH_4$ (Equation 5 or 6) in this fuel cell when hydrogen is consumed by the anodic reaction

$$H_2 \longrightarrow 2H^+ + 2e^- \quad (7)$$

As described in our previous study [6], one of the unique characteristics of the proton-conductor fuel cell is that hydrocarbons are not fully oxidized, while, with an oxide ion conductor, $CO_2$ is formed as a by-product in the oxidative coupling reaction [11]. Such studies for dehydrogenation or hydrogenation of some organic compounds are under way.

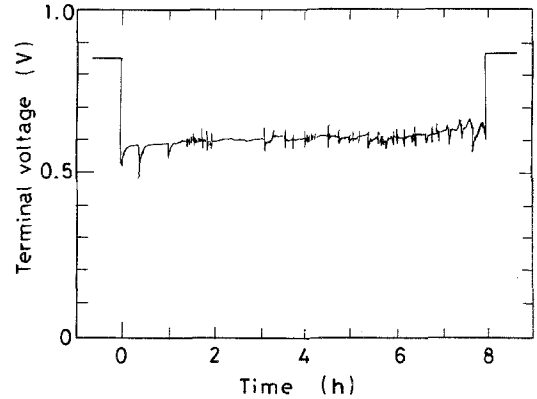


Fig. 3. Continuous discharge test of the methane fuel cell (Fig. 2) at constant current density of 70 mA cm$^{-2}$ at 1000° C. ($P_{H_2O}$ in fuel = 200 torr).

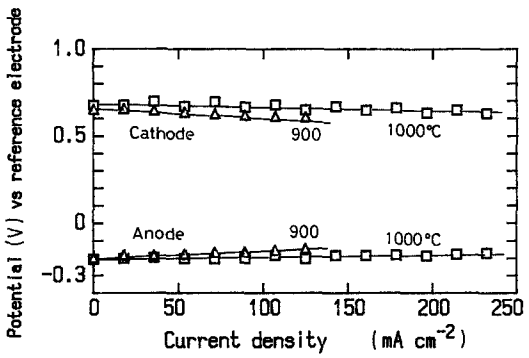


Fig. 4. Polarization characteristics of the electrodes in the same cell as in Fig. 2.

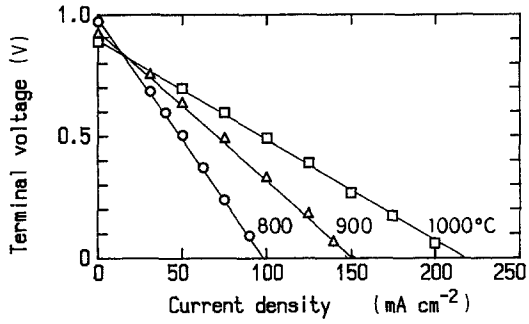


Fig. 5. Performance of the methanol fuel cell; $CH_3OH + H_2O +$ Ar, Pt|$SrCe_{0.95}Yb_{0.05}O_{3-\alpha}$|Pt, air ($CH_3OH:H_2O$ = 4:1 by volume, Ar flow rate = 40 ml min$^{-1}$, saturator temperature = 22° C, electrolyte thickness = 0.50 mm).

### 3.2. *Methanol fuel cell using argon saturated with $CH_3OH$*

As a fuel, methanol vapor carried with argon gas was supplied to the above cell. The fuel gas contained about 10% methanol vapor and 2–3% water vapor. The cell gave rise to a stable EMF of about 900 mV.

Typical cell performances are shown in Fig. 5. The cell also worked stably in this case. The current output was steady and the relation between the terminal voltage and the current density was linear at 800–1000° C.

Table 2 shows the composition of the exhaust gas from the anode compartment at open circuit. The exhaust gas contained $H_2$, CO, $CO_2$, $CH_4$ and unreacted $CH_3OH$. Judging from the composition of the gas, methanol vapor was almost fully pyrolyzed by 'internal reforming' above 900° C, while the decomposition rate was about 50% at 800° C. Since the $H_2$/CO ratio was about 2 above 900° C at open circuit, the following pyrolysis reaction might be dominant in the anode compartment

$$CH_3OH \longrightarrow 2H_2 + CO \qquad (8)$$

When dry argon was supplied to the cathode instead of air and direct current was passed through the electrolyte, hydrogen evolution was recognized at the cathode by gas chromatography. Figure 6 shows the plot of hydrogen evolution rate against current density at 800° C. The evolution rate is close to the theoretical calculated from Faraday's law. This indicates that the $SrCeO_3$-based ceramic electrolyte in this cell functioned as a proton conductor.

The polarization characteristics are shown in Fig. 7. The major limitation of the cell can be regarded as the resistance of the electrolyte. Although the concentration of hydrogen at the anode was not so high (Table 2), the anodic polarization was small within the current density examined (< 250 mA cm$^{-2}$). This may be somewhat anomalous because an anodic polarization due to diffusion limitation of hydrogen should occur to some extent in such a situation [12]. Then, we considered the anode reaction in detail.

*Table 2. Composition of exhaust gas from fuel compartment at open circuit: $CH_3OH + H_2O + Ar$, Pt |$SrCe_{0.95}Yb_{0.05}O_{3-\alpha}$| Pt, air ($CH_3OH:H_2O$ = 4:1 by volume, Ar flow rate = 60 ml min$^{-1}$, saturator temp. = 28° C)*

| Cell temp. (° C) | Composition (%) | | | |
|---|---|---|---|---|
| | $H_2$ | $CH_4$ | CO | $CO_2$ |
| 800 | 7.9 | trace | 3.3 | 0.1 |
| 900 | 15.8 | 0.3 | 8.1 | 0.1 |
| 1000 | 16.3 | 0.3 | 8.3 | 0.2 |

### 3.3. *The dependence of exhaust gas composition on discharge current in the methanol fuel cell*

In order to obtain information for the 'internal reforming' reaction on discharging the fuel cell, the change in the composition of the exhaust gas was analyzed. For this experiment, a closed-end-type tube of ceramic electrolyte (electrode area: about 6 cm$^2$) was used to discharge the cell at high current level. Argon gas, saturated with aqueous methanol at 40° C, was introduced into the cell at a flow rate of 30 ml min$^{-1}$. In this fuel gas, the partial pressures of $CH_3OH$ and $H_2O$ were about 0.2 and 0.03 atm, respectively [13]. Each gas flux was calculated as the product of the concentration and the total gas flow rate and plotted against the discharge current. Typical

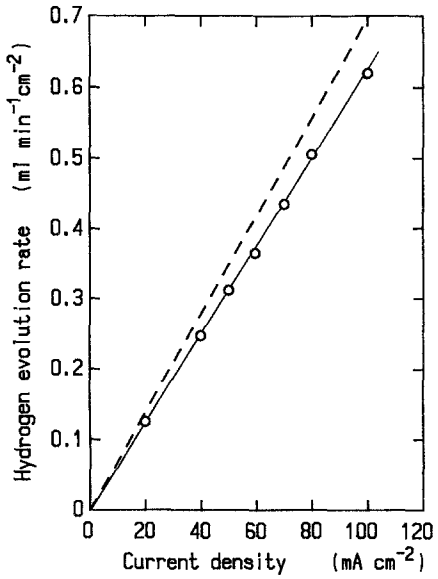


Fig. 6. Electrochemical extraction of hydrogen from the pyrolized gas of methanol at 800° C. Broken line shows the theoretical rate.

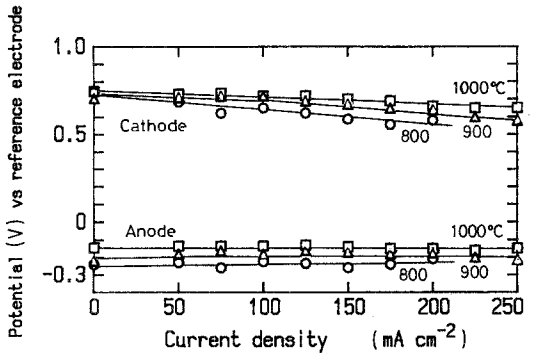


Fig. 7. Polarization characteristics of the electrodes in the same cell as in Fig. 5.

results are shown in Fig. 8 (horizontal axis is current instead of current density, because the electrode area was not so definite for this electrolyte).

As shown in (a) in Fig. 8, in the low current region, the hydrogen flux decreased with increasing discharge current at a rate close to the theoretical, because hydrogen must be consumed at the anode (Equation 7). However, in the high current region above 200 mA, the decrease in hydrogen flux did not obey Faraday's law. We also observed a decrease in the $CH_3OH$ flux and an increase in the $CO_2$ flux with increasing discharge current ((b) and (c) in Fig. 8). These results suggest that hydrogen consumed by the anodic reaction (Equation 7) might be made up by pyrolysis of $CH_3OH$ (Equation 8) and the water gas shift reaction (Equation 9).

$$H_2O + CO \rightleftarrows H_2 + CO_2 \qquad (9)$$

It may be a 'buffer effect', which relaxes the depletion of hydrgen at the anode. Due to such a 'buffer effect', the anodic polarization might not be so large in this cell.

As shown in (d) in Fig. 8, the CO flux decreased with increasing current at 800° C whereas at 900° C it was almost independent of discharge current and the utilization of CO was very low. This may be due to the decrease in the equilibrium constant with increasing temperature [14]. Another reason for this may be a low utilization level of the fuel in our test cell. Under such a condition, the change in hydrogen concentration was too small to cause a detectable change in the $CO_x$ concentration (Equation 9).

### 3.4. *Methanol fuel cell using direct vaporizer*

In the cell described above, we used argon gas as the carrier of methanol and water vapor. However, its hydrogen concentration at the anode was not so high (about 16% above 900° C). If a fuel with higher hydrogen partial pressure is introduced into the cell, the performance may be improved. For this purpose, we

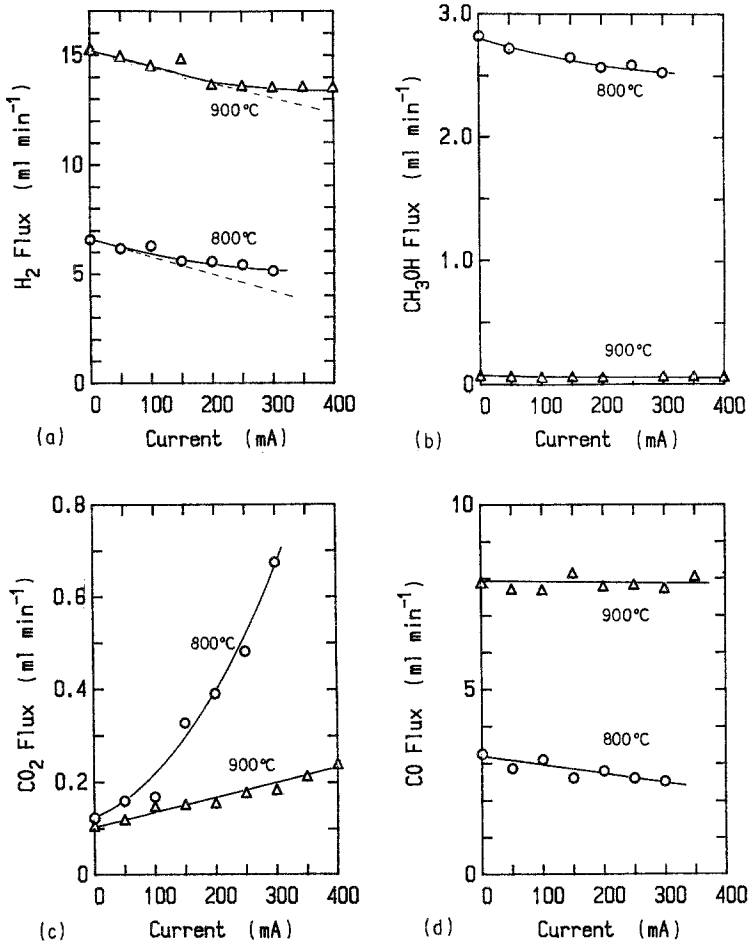


Fig. 8. Change in gas flux of (a) $H_2$, (b) $CH_3OH$, (c) $CO_2$ and (d) CO in the exhaust gas on discharging the methanol fuel cell. (Electrolyte = one end closed tube, Ar flow rate = 30 ml min$^{-1}$, saturator temperature = 40° C. Broken line in (a) shows the theoretical change in hydrogen flux according to Equation (7). Gas flux is shown in STP.)

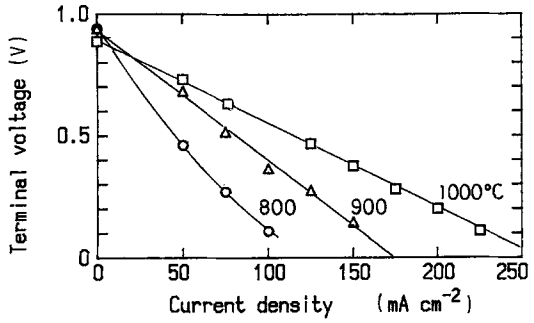


Fig. 9. Performance of $CH_3OH$–$O_2$ fuel cell using methanol vaporizer; $CH_3OH + H_2O$, $Pt|SrCe_{0.95}Yb_{0.05}O_{3-\alpha}|Pt$, $O_2$ ($CH_3OH$: $H_2O$ = 4:1 by volume, fuel feed rate = 0.05 ml min$^{-1}$, electrolyte thickness = 0.50 mm).

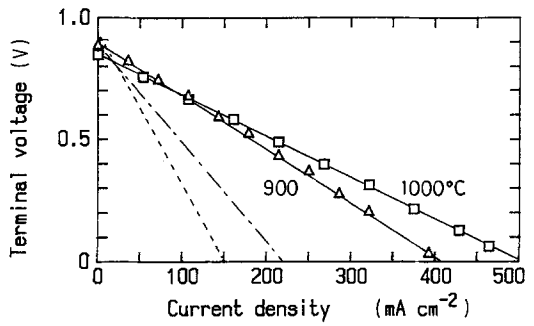


Fig. 10. Performance of the methanol fuel cell using $BaCeO_3$-based electrolyte; $CH_3OH + H_2O$ + Ar, $Pt|BaCe_{0.90}Nd_{0.10}O_{3-\alpha}|Pt$, air ($CH_3OH:H_2O$ = 4:1 by volume, Ar flow rate = 40 ml min$^{-1}$, saturator temperature = 22° C, electrolyte thickness = 0.50 mm). Performances of similar cell using $SrCe_{0.95}Yb_{0.05}O_{3-\alpha}$ electrolyte (Fig. 5) are shown by broken line; – – – 900° C, – – – 1000° C.

employed a vaporizer heated by waste heat from the electric furnace. Aqueous methanol was fed to the vaporizer at a rate of about 0.05 ml min$^{-1}$ by a microfeeder and was evaporated directly. In order to obtain sufficient hydrogen content, the $CH_3OH/H_2O$ mole ratio was chosen to be about 2, which is in excess of the stoichiometry (1:1) for full decomposition as obtained from Equations 8 and 9

$$CH_3OH + H_2O \rightleftharpoons 3H_2 + CO_2 \qquad (10)$$

This type of fuel cell worked stably. Figure 9 shows the performance of such a cell. Although the hydrogen concentration at the anode was high (about 60% at the outlet), the cell performance was not so good compared with the previous cell with carrier gas. This means that the cell peformance is limited not by the concentration polarization at the anode, but by other factors such as ohmic resistance of the electrolyte and polarization at the cathode. However, direct evaporation of aqueous methanol may be a promising method for a practical fuel cell under high current density operation (high fuel utilization).

### 3.5. *Methanol fuel cell with $BaCeO_3$-based electrolyte*

As reported previously, $BaCe_{0.90}Nd_{0.10}O_{3-\alpha}$ is also a good proton conductor in a hydrogen-containing atmosphere at elevated temperature [2].

We applied this ceramic as the solid electrolyte for the methanol fuel cell described above. Typical performances are shown in Fig. 10. A steady and stable current could be drawn from the cell. Because the ionic conductivity of $BaCe_{0.90}Nd_{0.10}O_{3-\alpha}$ was about two or three times higher than that of $SrCeO_3$-based ceramics [2], the voltage drop due to the ohmic resistance of the electrolyte was small. The terminal voltage was about 0.5 V at 200 mA cm$^{-2}$ at 1000° C, which was an appreciably higher performance compared with our previous cell (broken line in Fig. 10). However, in $BaCeO_3$-based ceramics, we observed an oxide ionic conduction besides protonic conduction in the high temperature region [2]. Detailed studies for such conduction properties as well as the performance of the fuel cell are in progress in our laboratory.

## 4. Conclusions

With proton-conducting solid electrolytes based on $SrCeO_3$, high temperature $C_1$-gas fuel cells could be constructed. The cell worked stably when a $C_1$ gas such as methanol or methane was used as the fuel together with an appreciable amount of water vapor. Electrode polarizations were small at 1000° C. However, a cathodic polarization became significant as the temperature decreased.

Due to its high conductivity, the $BaCeO_3$-based ceramic is also a promising material for an electrolyte of fuel cell, although the conduction is not only protonic but partially oxide ionic.

## References

[1] H. Iwahara, T. Esaka, H. Uchida and N. Maeda, *Solid State Ionics* **3/4** (1981) 359.
[2] H. Iwahara, H. Uchida, K. Ogaki and K. Ono, *J. Electrochem. Soc.* **135** (1988) 529.
[3] H. Iwahara, H. Uchida and T. Esaka, *Prog. Batt. Solar Cells* **4** (1982) 279; H. Iwahara, H. Uchida and N. Maeda, *J. Power Sources* **7** (1982) 293.
[4] H. Iwahara, H. Uchida and S. Tanaka, *Solid State Ionics* **9/10** (1983) 1021.
[5] H. Uchida, S. Tanaka and H. Iwahara, *J. Appl. Electrochem.* **15** (1985) 93.
[6] H. Iwahara, H. Uchida and S. Tanaka, *ibid.* **16** (1986) 663.
[7] H. Iwahara, T. Esaka, H. Uchida, T. Yamauchi and K. Ogaki, *Solid State Ionics* **18/19** (1986) 1003.
[8] D. C. Fee, S. A. Zwick and J. P. Ackerman, US DOE Rep. (CONF-8308120-1) (1983).
[9] M. Krumpelt, C. M. Cook, R. D. Pierce and J. P. Ackerman, US DOE Rep. (CONF-840201-3) (1984).
[10] M. Krumpelt, E. J. Daniels, C. B. Dennis and R. D. Pierce, 172nd Meeting, The Electrochem. Soc., Extended Abstracts, Hawaii (1987) p. 261.
[11] K. Otsuka, S. Yokoyama and A. Morikawa, *Chem. Lett.* (1985) 319.
[12] H. Uchida, K. Morimoto and H. Iwahara, The 28th Battery Symposium in Japan, Abstracts, Tokyo (1987) p. 25.
[13] C. J. West, 'International Critical Tables', McGraw-Hill, New York (1930) Vol. V, p. 290.
[14] C. J. West, *ibid*, Vol. VII, p. 243.